Meteorol Atmos Phys (2013) 120:73–82
DOI 10.1007/s00703-013-0239-7

ORIGINAL PAPER

Least-squares harmonic estimation of the tropopause parameters using GPS radio occultation measurements

Mohammad Ali Sharifi · Ali Sam Khaniani · Salim Masoumi · Torsten Schmidt · Jens Wickert

Received: 12 March 2012 / Accepted: 12 February 2013 / Published online: 2 March 2013

Abstract In order to investigate temporal variations of the tropopause parameters, Least-Squares Harmonic Estimation (LS-HE) is applied to the time series of the tropopause temperatures and heights derived from Global Positioning System Radio Occultation (GPS RO) atmospheric profiles of CHAMP, GRACE and COSMIC missions from January 2006 until May 2010 in different regions of Iran. By applying the univariate LS-HE to the completely unevenly spaced time series of the tropopause temperatures and heights, annual and diurnal components are detected together with their higher harmonics. The multivariate LS-HE estimates the main periodic signals, particularly diurnal and semidiurnal cycles, more clearly than the univariate LS-HE. Mixing in the values of the tropopause height and temperature is seen to occur in winter at lower latitudes (around 30°) as a result of subtropical jet, and in summer at higher latitudes (36°–42°) as an effect of subtropical high. A bimodal pattern is observed in the frequency histograms of the tropopause heights, in which the primary modes for the southern and northern parts of Iran correspond to subtropical and extratropical heights, respectively.

Responsible editor: C. Simmer.

M. A. Sharifi · A. Sam Khaniani (✉) · S. Masoumi
Department of Surveying and Geomatics Engineering, University College of Engineering, University of Tehran, North Kargar Ave., P.O. Box 11365-4563, Tehran, Iran
e-mail: ali.sam@ut.ac.ir

T. Schmidt · J. Wickert
Department of Geodesy and Remote Sensing, German Research Center for Geosciences (GFZ), Telegrafenberg, 14473 Potsdam, Germany

1 Introduction

The tropopause layer, as the transition layer between the troposphere and the stratosphere, has a critical role in the climatology and the atmospheric cycles (Holton et al. 1995; Sausen and Santer 2003; Santer et al. 2004; Schoeberl 2004; Li et al. 2010). The tropopause is generally affected by the tropospheric and stratospheric temperatures (Schmidt et al. 2010; Hall et al. 2011). Due to the location of the tropopause, any change in the physical, chemical or thermal characteristics of the stratosphere or the troposphere results in the variation of the tropopause parameters (Mehta 2010).

The tropopause parameters change in an extended time scale from a year to a few hours. Plenty of research has been done on the long-term variations of the tropopause including annual, inter-annual and monthly changes (Reid and Gage 1985, 1996; Krishna Murthy et al. 1985; Randel et al. 2000; Hashiguchi et al. 2006; Hall et al. 2011). The diurnal and sub-diurnal variations have been also studied by, e.g., Revathy et al. (2001), Son and Lee (2007) and Li et al. (2010).

In addition to the time scale variety in studying the tropopause parameters, data used for the studies have been different. Krishna Murthy et al. (1985) used 9 years of the radiosonde measurements in 11 stations at the geographic latitude range of 8.5°–28.6° N to investigate annual and semiannual variations of the tropical tropopause parameters. Based on the radiosonde data in Wuhan between 11 and 16 January 2006, the diurnal variations of the tropopause temperatures and heights were clearly demonstrated by Li et al. (2010). Revathy et al. (2001) used Mesosphere Stratosphere Troposphere (MST) radar, and observed an obvious diurnal cycle of the Cold Point Tropopause (CPT). The operational rawinsonde data in Indonesia (Hashiguchi

et al. 2006) and SOUSY VHF radar in Svalbard (Hall et al. 2011) were used to detect the temporal changes of the tropopause temperatures and heights.

On top of the above data sources, Global Positioning System Radio Occultation (GPS RO) was proposed and applied for the remote sensing of the atmosphere to generate profiles of refractivity, pressure, temperature and water vapor. This technique depends on the precise measurements of the phases of the two GPS frequencies by a receiver onboard a Low Earth Orbiting (LEO) satellite. Signal bending is derived from the excess phase delay in the receiver, and the bending can be interpreted based on the changes of the atmospheric refractivity (Wickert et al. 2009). Several works have studied radio occultation and its power, accuracy and advantages such as long-term stability, global coverage, high vertical resolution and any-weather performance (Gorbunov and Sokolovisky 1993; Hajj et al. 1994; Gorbunov 1993; Kursinski et al. 1997; Mortensen and Hoeg 1998; Kursinski et al. 2000; Healy 2001). Recent studies have estimated the observational errors of the temperature profiles produced by RO to be between 0.7 and 1 K at the altitudes of 8–25 km (Steiner et al. 2011). Therefore, as this altitude range includes the height of the tropopause, RO temperature profiles with altitude resolutions of about 100 m (Leroy et al. 2012) can be of enough precision for deriving the tropopause heights and temperatures.

Least-Squares Harmonic Estimation (LS-HE) was introduced by Amiri-Simkooei (2007) as a frequency analysis method applicable to the unevenly spaced series. The method is used here to investigate periodic patterns of the tropopause parameters and to detect the common signals in all the time series of the tropopause heights and temperatures.

The data used for the study is introduced in Sect. 2. The formulations for the LS-HE are described in Sect. 3. In Sects. 4 and 5, the time series of the tropopause parameters are displayed, the LS-HE is applied to them, and the periodic behavior of the layer and its main frequencies are studied. Summary and conclusions are given in the last section.

2 Data

Since there are few radiosonde stations in the region of Iran, GPS RO measurements can be used instead of radiosonde data for the atmospheric studies. RO data from the three satellite missions of CHAMP (CHAllenging Minisatellite Payload), GRACE (Gravity Recovery and Climate Experiment) and COSMIC (Constellation Observing System for Meteorology, Ionosphere, and Climate) retrieved from the University Corporation for Atmospheric Research (UCAR) (http://www.cosmic.ucar.edu) are used in this study. RO temperature profiles from 32 months of CHAMP (January 2006 until September 2008), 39 months of GRACE (March 2007 until May 2010) and 47 months of COSMIC (July 2006 until May 2010) observations are collected in the region of Iran with the geographic latitudes of 24°–42° and the geographic longitudes of 43°–65°.

Presence of the mountainous areas around Alborz Mountains in the north and Zagros Mountains in the west, a desert area in the central part, the short distance of the southern parts from the equator and the existence of Caspian and Oman seas in the north and south of Iran lead to variable climatic conditions, and therefore, an expected variable tropopause structure in the region under study. Consequently, based on the geographic properties, particularly the topographic conditions, the region is divided latitudinally into three regions and longitudinally into two regions. Figure 1 displays the digital elevation model of the region and the six defined divisions.

The tropopause temperatures and heights are derived from RO temperature profiles. Among the several definitions for determining the location of the tropopause (Pan et al. 2004), Lapse Rate Tropopause (LRT) defined by the World Meteorological Organization (WMO) (WMO 1957) is used. Details on the determination of the height and other tropopause parameters using the lapse rate temperature can be found in Schmidt et al. (2005) and Wickert et al. (2006).

3 Least squares harmonic estimation

Consider the linear model of observation equations for the time series $y(t)$:

$$E(y) = Ax,\ D(y) = Q_y \tag{1}$$

where A is the $m \times n$ design matrix, Q_y is the $m \times m$ covariance matrix of the $m \times 1$ vector of observables y, x is the n-vector of the unknown parameters, and D and E are, respectively, the expectation and dispersion (or covariance) operators. The linear model needs to be improved by adding a set of sinusoidal signals to express the periodic patterns in the series. This will improve the functional model of Eq. (1).

The periodic signals are added to the functional model. Hence, the functional model takes the form:

$$E(y) = Ax + \sum_k (a_k \cos \omega_k t + b_k \sin \omega_k t),\ D(y) = Q_y \tag{2}$$

where a_k, b_k and ω_k are the unknown real numbers. The matrix form of the Eq. (2) is written as the following equation:

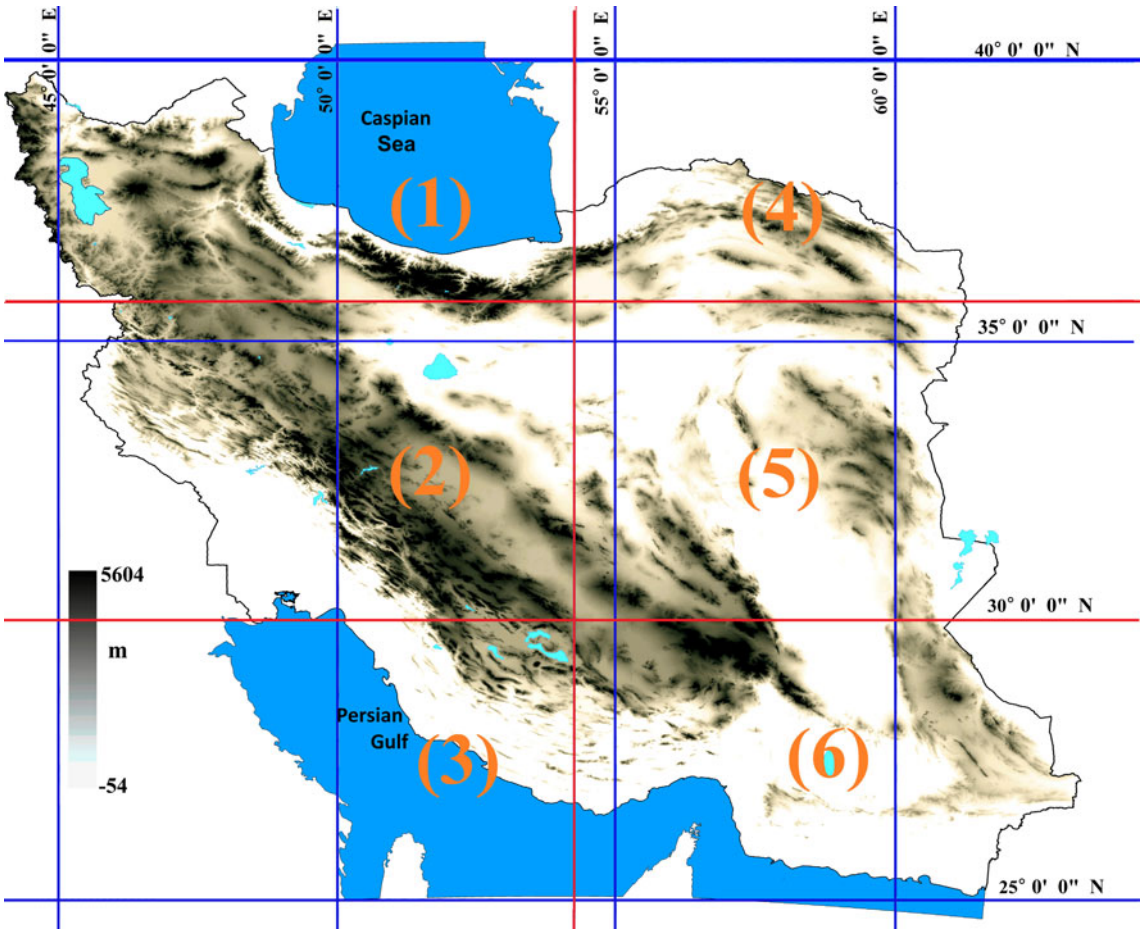

Fig. 1 Digital elevation model of Iran, and the six defined regions

$$E(y) = Ax + A_k x_k,\ D(y) = Q_y \tag{3}$$

where A_k is a matrix with two columns corresponding to the frequency ω_k of the sinusoidal function:

$$A_k = \begin{bmatrix} \cos \omega_k t_1 & \sin \omega_k t_1 \\ \vdots & \vdots \\ \cos \omega_k t_m & \sin \omega_k t_m \end{bmatrix}, \quad x_k = \begin{bmatrix} a_k \\ b_k \end{bmatrix} \tag{4}$$

Using the recursive equation proposed by Amiri-Simkooei et al. (2007), the discrete frequencies for which the powers will be estimated are sampled as follows:

$$T_{j+1} = T_j \left(1 + \frac{\alpha T_j}{T}\right),\ \alpha = 0.2,\ j = 1, 2, \ldots \tag{5}$$

In the above equation, T is the total time span of the time series which is equal to 1,610 days here. T_1 is the shortest period to be examined, and is selected as $1/24$ days. The smallest frequency to be examined is $\omega_{\text{Min}} = 2\pi/T$.

Assuming the frequencies to be given by Eq. (5) and the time series to contain only white noise ($Q_y = I$), the spectral power for each frequency ω_k is determined as follows for a zero mean stationary random process $y(t)$ (Amiri-Simkooei and Asgari 2011):

$$P(\omega_k) = y^T A_k (A_k^T A_k)^{-1} A_k^T y \tag{6}$$

Equation (6) is called the solution for the univariate harmonic estimation. If there are several time series with the linear models for which the design (A) and the covariance (Q_y) matrices are identical, the problem can be solved by a multivariate harmonic estimation (Amiri-Simkooei and Asgari 2011). With the assumption that no correlation exists between the different time series, the solution for the multivariate harmonic estimation is given by:

$$P(\omega_k) = \sum_{i=1}^{r} \frac{y^T A_k (A_k^T A_k)^{-1} A_k^T y}{\sigma_{ii}} \tag{7}$$

where r is the number of time series, and σ_{ii} is the standard deviation for the ith time series. Equation (7) is in fact the weighted stacked power spectrum of the individual power spectra (Amiri-Simkooei and Asgari 2011).

An Advantage of LS-HE over the ordinary Fourier spectral analysis is that it is limited neither to the evenly spaced data nor to integer frequencies. Some other forms of Fourier transform are also applicable to unevenly spaced data (Vanicek 1971; Lomb 1976; Scargle 1989, 1997); however, by LS-HE, one can include the linear trend and the covariance matrix as the deterministic and the stochastic models in the analyses, which is not possible by any previously introduced methods. Furthermore, the multivariate LS-HE improves the precision of the spectral power, which is a unique feature of this method.

4 Temporal variations of the tropopause parameters

The separation between the tropical and midlatitude meteorology regimes has been clearly seen over Iran where the upper tropopause is affected by different types of atmospheric phenomena (e.g., Hudson et al. 2003). During winter, some types of fronts enter the region from the south, southwest and west (around 30° latitude), which are associated with the subtropical jet and result in heavy rainfall in Iran. During summer, thermal low forms below the subtropical high (approximately in 37°–43° latitudes) due to continental features over the mainland.

Using RO data from CHAMP, GRACE and COSMIC missions from January 2006 until May 2010 and based on the definition from WMO (1957), the time series for the LRT heights and temperatures are formed for the six defined regions (see Fig. 1). The time series of the tropopause heights and temperatures are illustrated in Figs. 2 and 3, respectively. Since there are only CHAMP RO data for the first 6 months of 2006, the time series have smaller amount of data for this period. The periodic behaviors of the tropopause parameters are clearly seen in the plots.

By looking at the variations of the tropopause height and temperature in Figs. 2 and 3 from a spatial perspective, the differences are clearly observed between regions 1, 2 and 3. Similar behaviors are, respectively repeated in regions 4, 5 and 6 as the first three regions, both in temperature and height. This shows the strong dependence of the tropopause features on the geographic latitude (which was also expressed by, e.g., Khandu et al. (2010)) and their independence from the geographic longitude and from the topography. In particular, regions 3 and 5 are completely different in longitude and in topography (see Fig. 1), but the behavior of the time series for these two regions are similar to each other as they are located in the same latitudinal range.

By looking at the time series for the tropopause height in region 1 (36°–42°), mixing (red ellipses in Fig. 2) is periodically observed in summer months. Considering the geographic latitude range of this region, this can be attributed to the presence of subtropical high in these latitudes. For the southern part of Iran (region 3 with the latitudes 24°–30°), the mixing in the values of the tropopause height occurs in winter months, which can be attributed to the effect of subtropical jet. As the subtropical jet acts in around 30° latitude, the mixing in region 2 (30°–36°) is also observed in winter months.

As can be seen in Fig. 3, the tropopause temperature is at its peak when the tropopause height is minimum, and it has its smallest values when the height is maximum. However, mixing in the temperature time series occurs at the same times as in the height time series.

In order to investigate the statistical properties of the tropopause height, the frequency histograms of the tropopause heights are displayed for the six regions in Fig. 4. As seen in this figure, the histograms in all the six regions are distributed in bimodal forms. They are similar to bimodal densities of the tropopause height which have been obtained from the radiosonde stations (Seidel and Randel 2007). For the northern regions (regions 1 and 4), the bimodal density has two modes where 10.5 km is the primary mode. For the middle regions (regions 2 and 5), the profiles around both modes (11.5 and 16.5 km) are distributed in a nearly homogeneous pattern. Finally in the southern regions (regions 3 and 6), the dominant tropopause height is concentrated around 16.5 km. The primary mode in the southern regions is comparable with the subtropical tropopause height where that of the northern regions is close to the extratropical tropopause height.

Again, it is clear that there is no significant difference in the histograms for the regions with similar latitudes but different longitudes. The independence of the results from the longitude (which was also seen in Figs. 2 and 3) allows the elimination of the longitudinal divisions. Thus, the whole region can be divided only into three latitudinal zones. Statistical properties of the time series for each of these new zones are presented in Table 1.

As seen in the second column of Table 1, the RO data points are distributed in a quite homogenous pattern between the latitudinal zones. Furthermore, it is clear from the third column that the mean tropopause height is lower at higher latitudes, which is consistent with previous studies (e.g., Khandu et al. 2010).

5 Harmonic characterization of the tropopause

By applying the method of LS-HE on the time series of the tropopause heights and temperatures at different geographic latitudes, the periodic behavior and the main components included in the series are detected. After sampling the discrete frequencies by Eq. 5, the spectral power is computed for the unevenly spaced time series

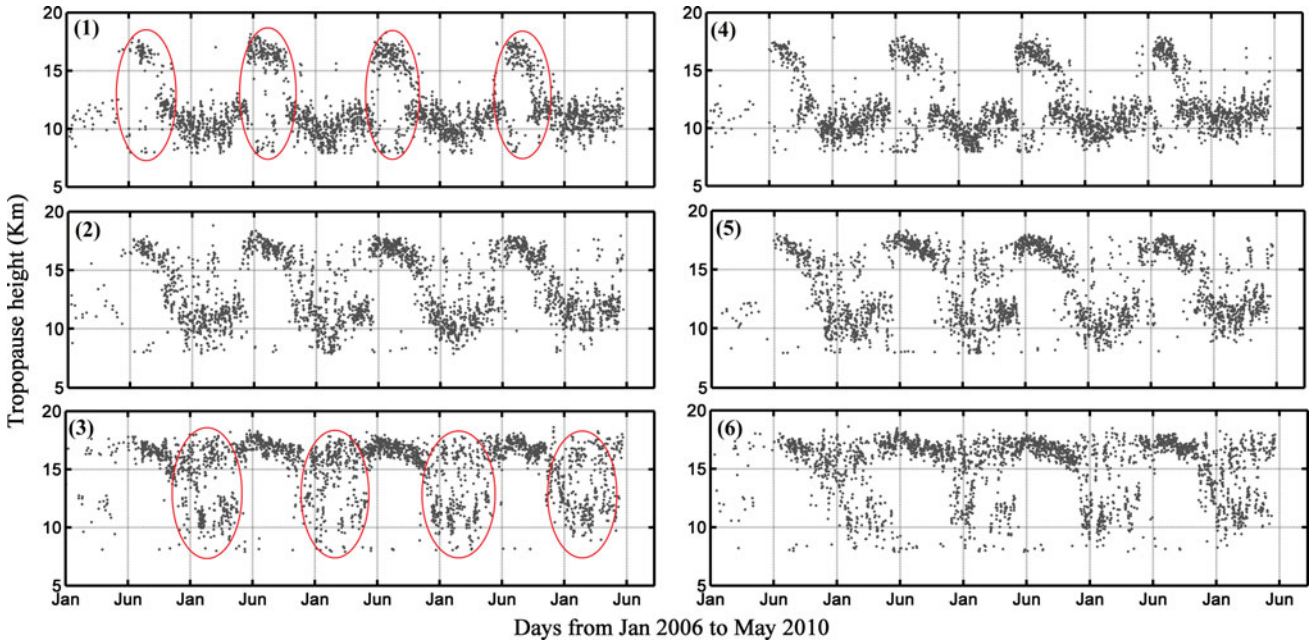

Fig. 2 The time series of the tropopause heights in the six defined regions of Iran from January 2006 until May 2010. The numbers in the *upper-left corner* of the plots indicates the spatial regions depicted in Fig. 1. The *red ellipses* show the occurrence of mixing (color figure online)

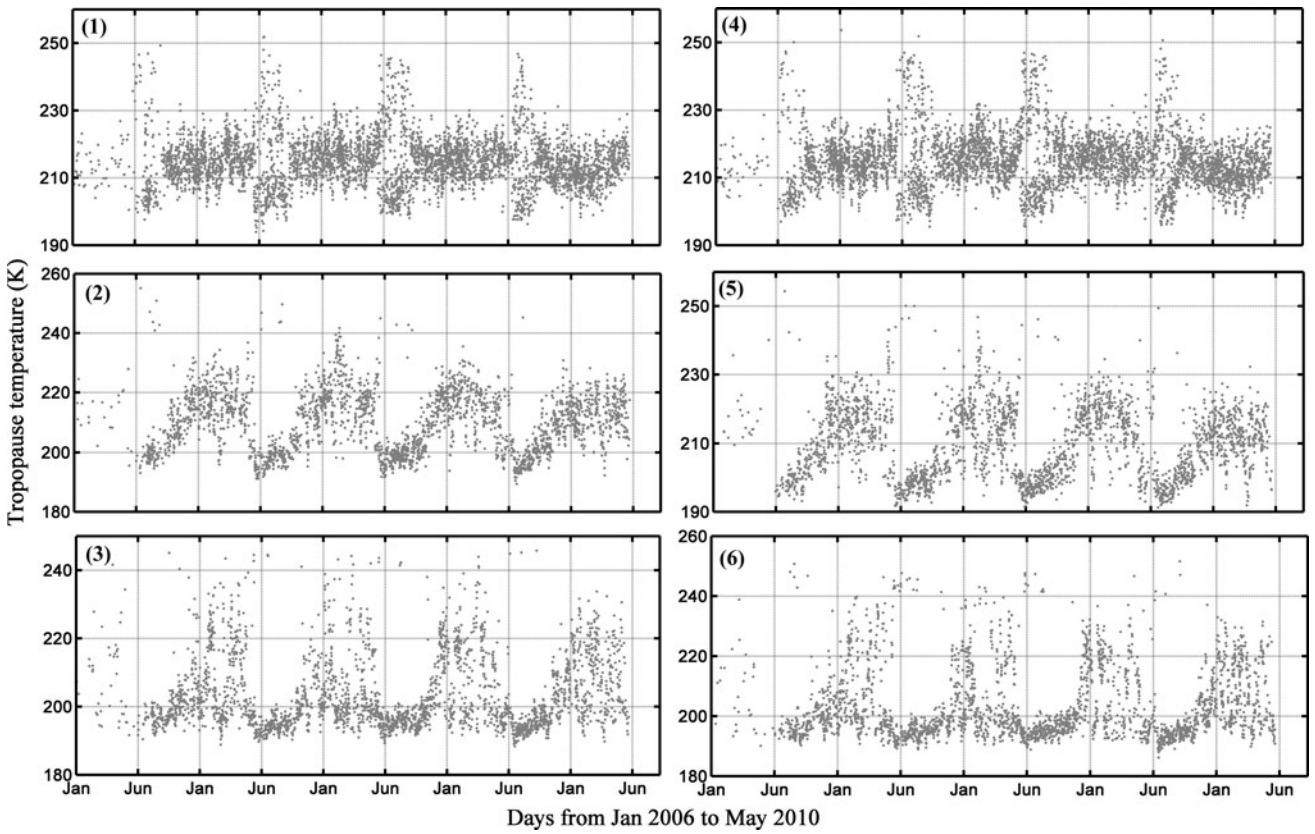

Fig. 3 The time series of the tropopause temperatures in the six defined regions of Iran from January 2006 until May 2010. The numbers in the *upper-left corner* of the plots indicate the spatial regions depicted in Fig. 1 (color figure online)

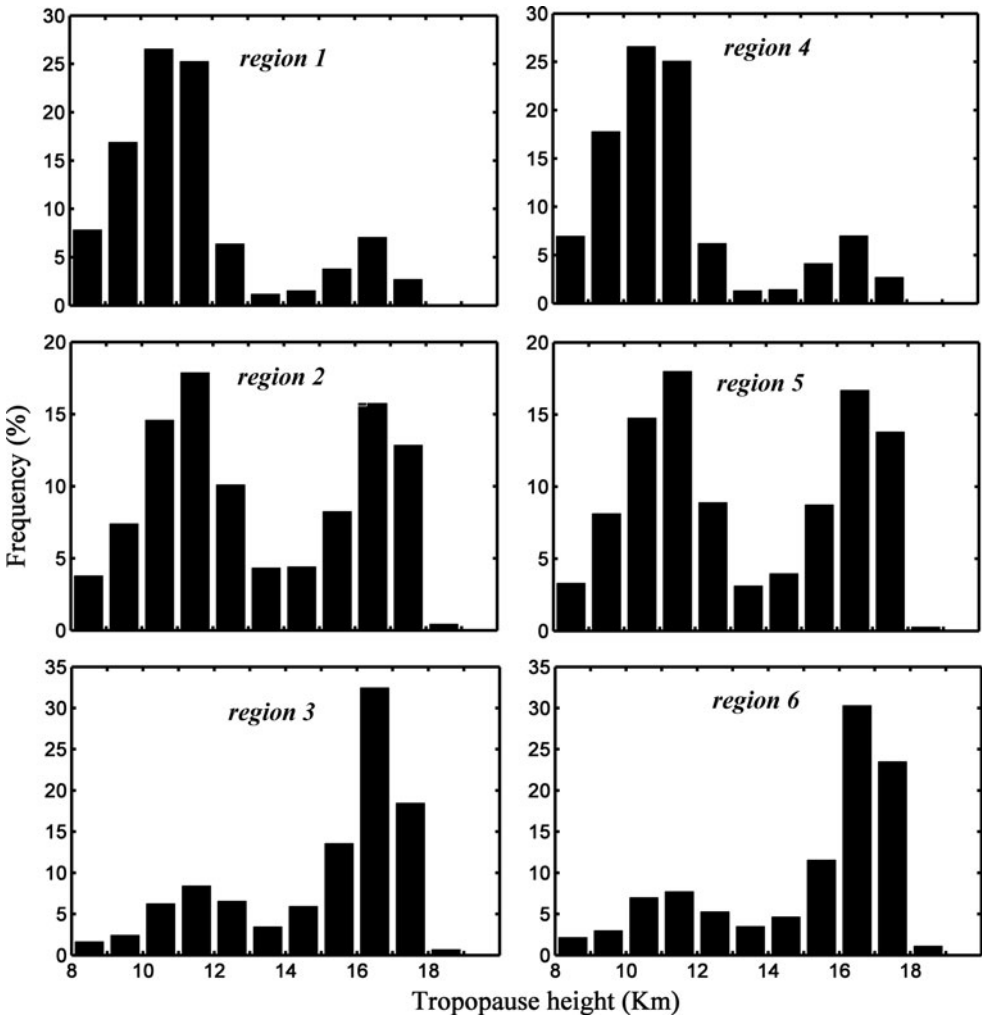

Fig. 4 Frequency histograms of the tropopause heights for the defined regions

Table 1 Statistical characteristics of the tropopause time series in the three latitudinal zones

Reigns	Data points	Mean (H_{trop}) (km)	Mean (T_{trop}) (K)	SD (H_{trop}) (km)	SD (T_{trop}) (K)	Lat (°)
1	6,839	11.8228	214.3886	2.5308	8.0262	36–42
2	6,227	13.3178	210.3761	2.8654	10.1335	30–36
3	6,602	14.9743	203.848	2.559	11.3968	24–30

using Eq. 6. Power spectra calculated for each time series (in the three defined latitudinal zones) are displayed in Fig. 5. The normalized univariate least-squares spectra for the time series of the tropopause heights and temperatures are shown at the left and right, respectively. The vertical dashed lines indicate the annual, sub-annual, diurnal and sub-diurnal signals.

As can be seen from Fig. 5, the annual signal together with its higher harmonics (1 year/n, $n = 1, 2, 3, \ldots$) are the dominant components in the time series of both the tropopause heights and temperatures. It is also observed that the annual cycle is stronger than the semiannual one by an approximate factor of two, which is consistent with the previous analyses on the temporal variations of the tropopause parameters (e.g., Krishna Murthy et al. 1985; Hashiguchi et al. 2006).

The periodic components of 24 h/n ($n = 1, 2, \ldots, 24$) are also present in the tropopause heights and temperatures, of which the most significant ones are the diurnal and semidiurnal signals. The diurnal cycle is directly related to the surface heating as described by Reid and Gage (1985). It should be noted that the higher harmonics of the main components do not necessarily need physical interpretations. They can be explained by the theory of series expansion of periodic functions. A periodic function with period of T can be written as an infinite sum of sine and

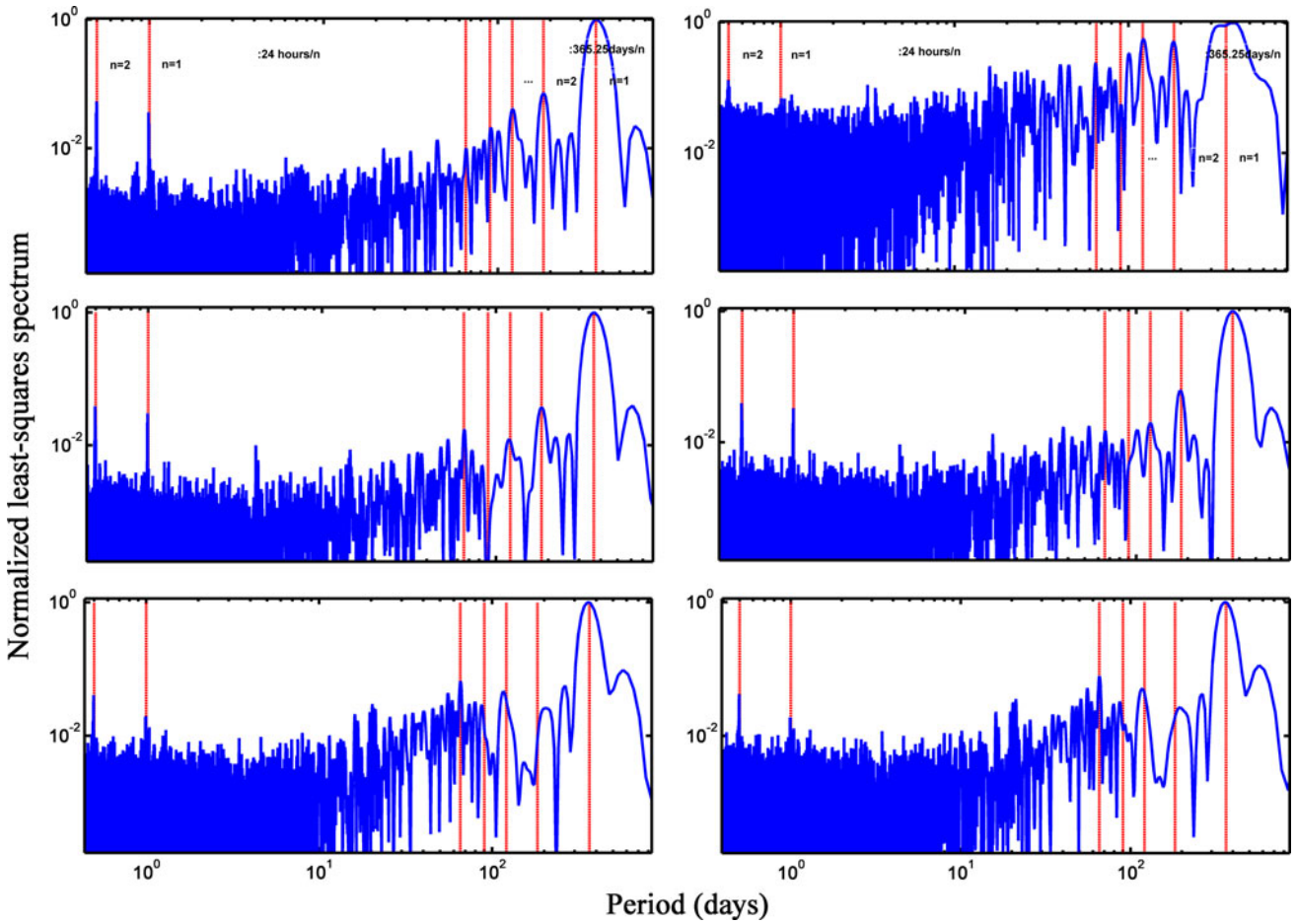

Fig. 5 Normalized least-squares power spectra for the time series of the tropopause heights (*left*) and temperatures (*right*) in the three latitudinal zones of Iran from January 2006 until May 2010. The *vertical dashed lines* indicate the annual and diurnal signals together with their higher harmonics

cosine functions on the interval $[-T/2, T/2]$, and the higher harmonics of a component are Fourier decomposition of the component into a truncated sum of sine and cosine functions (Amiri-Simkooei and Asgari 2011). Therefore, the sub-diurnal peaks could be explained as Fourier decomposition of the diurnal function.

The influencing factors on the position of the tropopause are mostly the ozone density and the surface air temperature (Santer et al. 2003; Zängl and Hoinka 2001; Hall et al. 2011); hence, the annual and diurnal periods and their higher harmonics, which are dominant in the LS-HE spectra, are probably related to the variations of these factors. However, it should be noted that the phase information is also needed to investigate the dependency of the tropopause height on the controlling factors. Hall et al. (2011) identified a phase-shift between the surface temperature and tropopause response, and no phase difference between tropopause minimum and ozone column density maximum.

The diurnal peaks are less clear in the power spectra, compared to the annual cycles. The diurnal and semidiurnal peaks are not clearly estimated in some of the periodograms, such as the spectra for the time series of the tropopause heights and temperatures for zones 1 and 3. Low temporal resolution of the data used may be a cause for this problem. To illustrate the temporal resolution of the data in each latitudinal zone, Fig. 6 shows the time gaps between consecutive measurements for each time series. The peaks present in the plots indicate large time gaps between the data. Because there were only CHAMP measurements available in the first 6 months of 2006, the largest time gaps happened in this time interval, reaching a maximum of 12 days.

A solution to cover for the time gaps in each time series with the data available by other series in the other zones is to use the multivariate LS-HE described in Sect. 3. This way, when there is a large time gap in a region, the measurements available for the other regions can be used to cover for the data gap. In addition, the standard deviation of each time series (see Table 1) is used in the multivariate LS-HE as a determining factor for weighting each series in the computation of the final spectrum. In other words, the

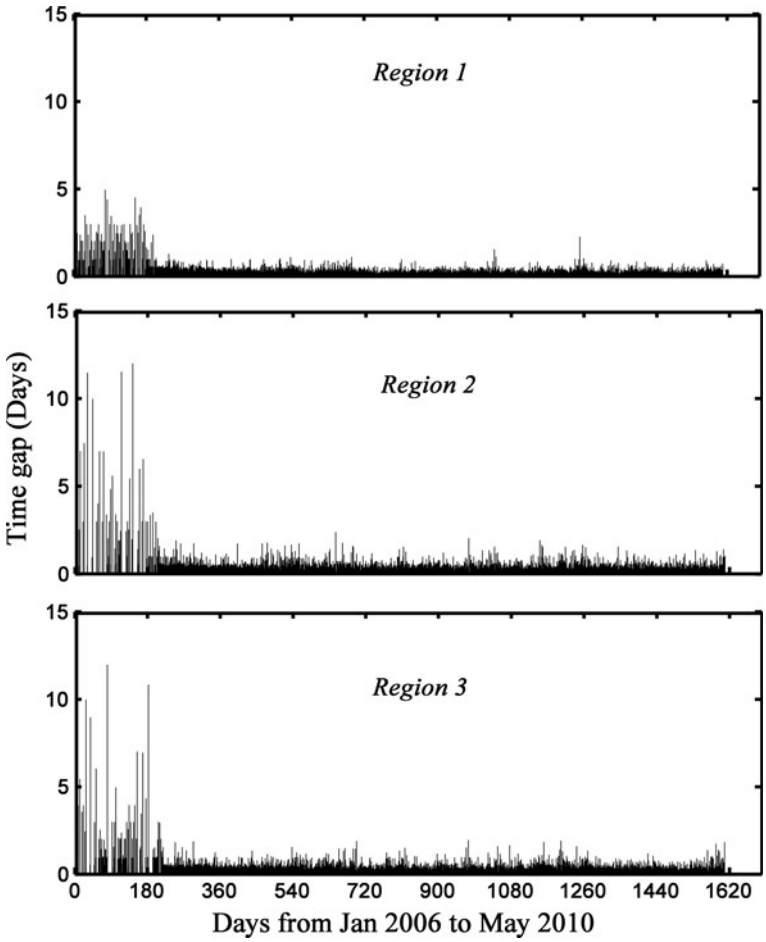

Fig. 6 Time gaps between consecutive measurements for each time series in the three latitudinal zones from January 2006 until May 2010

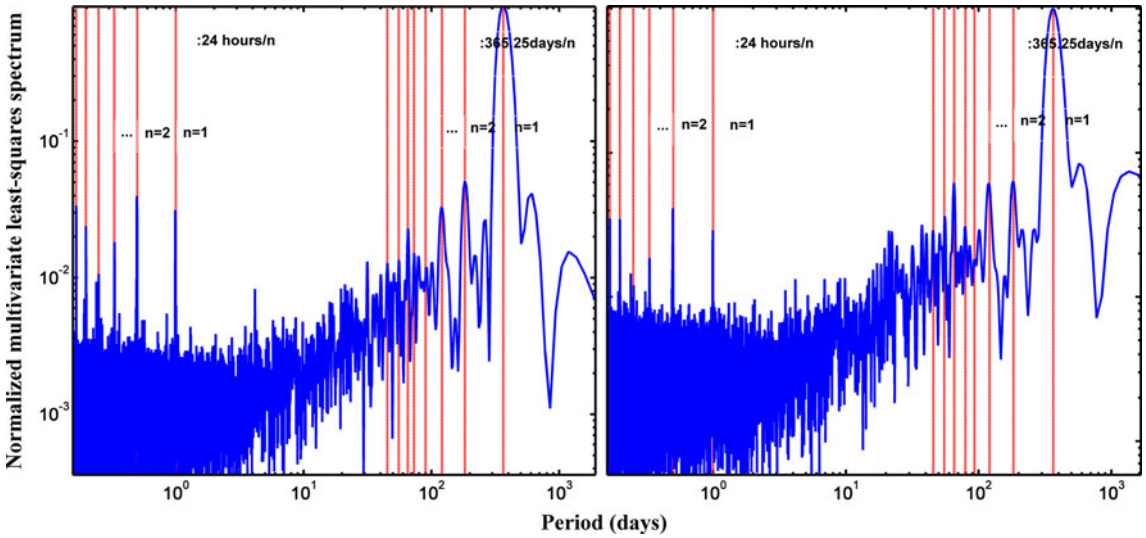

Fig. 7 Multivariate least-squares power spectra for the time series of the tropopause heights (*left*) and temperatures (*right*) from January 2006 until May 2010 estimated using the time series of the three latitudinal zones ranging from 24° to 42° latitude and 43° to 65° longitude. The *vertical dashed lines* indicate the annual and diurnal signals together with their higher harmonics

time series with larger variances have smaller contributions in the calculation of the multivariate power spectrum. The multivariate least-squares power spectra estimated using the time series of the three latitudinal zones are illustrated in Fig. 7. The results for the tropopause heights and temperatures are shown at the left and right, respectively.

It is inferred from Fig. 7 that the annual and sub-annual cycles are clearly observed as the main components of the tropopause parameters. Moreover, it can be observed that the multivariate LS-HE estimates the short-term periods (i.e. the diurnal and sub-diurnal cycles) more efficiently than the univariate power spectra of Fig. 5. Unlike the univariate LS-HE, the multivariate spectra clearly show both the long-term and short-term components. A reason for this is that the multivariate LS-HE uses the variances of the different series for weighting the series in the estimation of the spectra. Another reason for the better estimation of the main cycles by the multivariate LS-HE can be found by inspecting Fig. 6. The maximum time gaps between consecutive measurements in each time series is nearly randomly spread over the different latitudinal zones. Consequently, if all the times series are simultaneously used for the harmonic estimation (as used in the multivariate LS-HE), the time gaps in each time series are covered for by the data available by the other series at the same time interval. This way, the temporal resolution improves in the estimation of the dominant frequencies. As a result, the diurnal and semidiurnal variations are more clearly estimated by the multivariate LS-HE than by the univariate estimations of Fig. 5.

6 Summary and conclusions

The long-term and short-term temporal variations of the LRT temperatures and heights were studied in different regions of Iran by the use of the atmospheric profiles from January 2006 until May 2010 produced by the GPS RO technique. RO data from CHAMP, GRACE and COSMIC satellite missions were used for the study. The variations of the tropopause parameters had similar patterns in the identical ranges of the geographic latitudes, as previous research had shown the strong dependency of the tropopause heights on the geographic latitude.

It was inferred from the tropopause height and temperature time series that mixing occurs in winter in the latitudes between 24° and 36°, which can be attributed to the subtropical jet. At higher latitudes, mixing occurs in summer as a result of subtropical high. In addition, investigation of the frequency histograms of the tropopause heights illustrated a bimodal pattern, which is consistent with the earlier studies. The primary modes in the latitude ranges 24°–30° and 36°–42° were found to be around 16.5 km (in the order of subtropical tropopause height) and 10.5 km (in the order of extratropical tropopause height), respectively.

The least-squares harmonic estimation was applied to the time series of the LRT heights and temperatures, and the results were consistent with the previous analyses. By applying the univariate LS-HE, the annual signal and its higher harmonics were estimated as the dominant components, which is compatible with previous studies on the long-term variations of the tropopause (Krishna Murthy et al. 1985; Randel et al. 2000). Moreover, the annual component was estimated to be stronger than its higher harmonics, which confirms the previous works by, e.g., Krishna Murthy et al. (1985) and Hashiguchi et al. (2006). In addition to the long-term signals, the diurnal and semi-diurnal cycles were also estimated by the univariate LS-HE as the main short-term variations.

To overcome the time gaps in the time series of the different regions, the multivariate LS-HE was used to estimate the total power spectra for the tropopause heights and temperatures, which yielded more obvious annual and diurnal components together with their higher harmonics.

It should be noted that by applying the method of LS-HE to the evenly spaced radiosonde data, temporal variations of the tropopause parameters may be better investigated, since the climate is not really identical for the whole area of each of the three latitudinal zones specified in this study. In other words, by the use of this method on the long-term radiosonde time series in the different climatic regions, the dominant periodic components can be detected, and the variations can be compared for different regions. In addition, because of the high efficiency of the LS-HE in the frequency analysis of the completely unevenly spaced time series, use of this method is recommended for studying the periodic cycles of other RO-derived parameters related to the climatology and the stratosphere-troposphere exchange. With the future availability of COSMIC-2 RO data, the temporal resolutions of the time series will significantly improve, leading to better investigation of the periodicity in atmospheric parameters.

References

Amiri-Simkooei AR (2007) Least-squares variance component estimation: Theory and GPS applications. Ph.D Dissertation, Mathematical Geodesy and Positioning, Faculty of Aerospace Engineering, Delft University of Technology

Amiri-Simkooei AR, Asgari J (2011) Harmonic analysis of total electron contents time series: methodology and results. J GPS Solut. doi: 10.1007/s10291-011-0208-x (Online FirstTM)

Amiri-Simkooei AR, Tiberius CCJM, Teunissen PJG (2007) Assessment of noise in GPS coordinate time series: methodology and results. J Geophys Res 112:B07413. doi:10.1029/2006JB004913

Gorbunov ME (1993) Three-dimensional satellite refractive tomography of the atmosphere: numerical-simulation. J Radio Sci 31:95–104

Gorbunov ME and Sokolovskiy SV (1993) Remote sensing of refractivity from space for global observations of atmospheric parameters. Max-Planck-Institute fur Meteorologie Report No. 119, Hamburg, Germany

Hajj GA, Ibanez-Meier R, Kursinski ER, Romans LJ (1994) Imaging the ionosphere with the global positioning system. Int J Imag Syst Tech 5:174–184

Hall CM, Hansen G, Sigernes F, Kuyeng Ruiz KM (2011) Tropopause height at 78 N 16 E: average seasonal variation 2007–2010. J Atmo Chem Phys Disc. doi:10.5194

Hashiguchi NO, Yamanaka MD, Ogino S, Shiotani M, Sribimawati T (2006) Seasonal and interannual variations of temperature in the tropical tropopause layer (TTL) over Indonesia based on operational rawinsonde data during 1992–1999. J Geophys Res 111:D15110. doi:10.1029/2005JD006501

Healy SB (2001) Smoothing radio occultation bending angles above 40 km. Ann Geophys 19(4):459–478

Holton JR, Haynes PH, McIntyre ME, Douglass AR, Rood RB, Pfister L (1995) Stratosphere-troposphere exchange. Rev Geophys 33(4):403–439

Hudson RD, Frolov AD, Andrade MF, Follette MB (2003) The total ozone field separated into meteorological regimes. Part I: defining the regimes. J Atmos Sci 60:1669–1677

Khandu JL, Awange J, Wickert J, Schmidt T, Sharifi MA, Heck B (2010) GNSS remote sensing of the Australian tropopause. Climatic Change 105:1–22

Krishna Murthy BV, Parmeshwaran K, and Rose KO (1985) Temporal variation of the tropopause characteristics. J Atmos Sci 43:914–922, 986

Kursinski ER, Hajj GA, Schofield T, Linfield RP, Hardy KR (1997) Observing earth's atmosphere with radio occultation measurements using the Global Positioning System. J Geophys Res 102:23429–23465

Kursinski ER, Hajj GA, Leroy SS, Herman B (2000) The GPS radio occultation technique. Terr Atmos Ocean Sci 11(1):235–272

Leroy SS, Ao CO, Verkhoglyadova O (2012) Mapping GPS Radio Occultation data by Bayesian interpolation. J Atmos Ocean Tech 29(8):1062–1074

Li W, Ma H, Pang Z, Cai Z (2010) Diurnal variations of tropopause over Wuhan. International Conference on Industrial Mechatronics and Automation

Lomb NR (1976) Least squares frequency analysis of unevenly spaced data. Astrophys Space Sci 39(2):447–462. doi:10.1007/BF00648343

Mehta SK (2010) Studies on Characteristics of tropical tropopause. Ph.D Dessertation, Atmospheric Science, Department of Atmospheric Sciences, School of Marine Sciences, Cochin University of Science And Technology, Cohin-682016, Kerala, India

Mortensen MD, Hoeg P (1998) Inversion of GPS occultation measurements using fresneldi:raction theory. Geophys Res Lett 25(13):2441–2444

Pan LL, Randel WJ, Gary BL, Mahoney MJ, Hintsa EJ (2004) Definitions and sharpness of the extratropicaltropopause: a trace gas perspective. J Geophys Res 109(D23):D23103

Randel WJ, Wu F, Gaffen DJ (2000) Interannnual variability of the tropical tropopause derived from radiosonde data and NCEP reanalyses. J Geophys Res 105(D12):15509–15523

Reid GC, Gage KS (1985) Interannual variations in the height of tropical tropopause. J Geophys Res 90:5629–5635

Reid GC, Gage KS (1996) The tropical tropopause over the western Pacific: Wave driving, convection, and the annual cycle. J Geophys Res 101:21233–21241

Revathy K, PrabhakaranNayar SR, Krishna Murthy BV (2001) Diurnal variation of tropospheric temperature at a tropical station. Annales Geophysicae 19:1001–1005

Santer BD, Sausen R, Wigley TML, Boyle JS, AchutaRao K, Doutriaux C, Hansen JE, Meehl GA, Roeckner E, Ruedy R, Schmidt G, Taylor KE (2003) Behavior of tropopause height and atmospheric temperature in models, reanalyses, and observations: decadal changes. J Geophys Res 108(D1):4002. doi:10.1029/2002JD002258

Santer BD, Wigley TM, Simmons AJ, Kaallberg PW, Kelly GA, Uppala SM (2004) Identification of anthropogenic climate change using a second-generation reanalysis. J Geophys Res 109:D21104

Sausen R, Santer BD (2003) Use of changes in tropopause height to detect human influences on climate. Meteorol Z 12(3):131–136

Scargle JD (1989) Studies in astronomical time series analysis III.Autocorrelation and cross-correlation functions of unevenly sampled data. Astrophys J 343:874–887

Scargle JD (1997) Astronomical time series analysis: new methods for studying periodic and aperiodic systems. In: Maoz D, Steinberg A, Leibowitz EM (eds) Astronomical time series. Kluwer, Dordrecht, p 1

Schmidt T, Heise S, Wickert J, Beyerle G, Reigber C (2005) GPS radio occultation with CHAMP and SAC-C: global monitoring of thermal tropopause parameters. Atmos Chem phys 5:1473–1488

Schmidt T, Wickert J, Haser A (2010) Variability of the upper troposphere and lower stratosphere observed with GPS radio occultation bending angles and temperatures. Adv Space Res 46(2010):150–161. doi:10.1016/j.asr.2010.01.021

Schoeberl MR (2004) Extratropical stratosphere-troposphere mass exchange. J Geophys Res 109(D13):D13303

Seidel DJ, Randel WJ (2007) Recent widening of the tropical belt: evidence from tropopause observations. J Geophys Res 112:D20113. doi:10.10292007JD008861

Son SW, Lee S (2007) Intraseasonal variability of the zonal mean tropical tropopause height. J Atmos Sci 64:2695–2706

Steiner AK, Lackner BC, Ladstadter F, Scherllin-Pirscher B, Foelsche U, Kirchengast G (2011) GPS radio occultation for climate monitoring and change detection. Radio Sci 46:RSOD24. doi:10.1029/2010RS004614

Vanicek P (1971) Further development and properties of the spectral analysis by least-squares. Astrophys Space Sci 12(1):10–33. doi:10.1007/BF00656134

Wickert J, Beyerle G, Schmidt T, Healy SB, Heise S, Michalak G, Rothacher M (2006) GPS based atmospheric sounding with CHAMP: results achieved after four years. In: Proceedings of the 2005 EUMETSAT Meteorological Satellite Conference, Dubrovnik, Croatia

Wickert J, Michalak G, Schmidt T, Beyerle G, Cheng C, Healy S et al (2009) GPS radio occultation: results from CHAMP, GRACE and FORMOSAT-3/COSMIC. TerrAtmos Ocean Sci 20:35–50

WMO (1957) Definition of tropopause. World Meteorological Organisation, Geneva

Zängl G, Hoinka KP (2001) Thetropopause in the polar regions. J Climate 14:3117–3139